

# Discovery of Potent Triple Inhibitors of Both SARS-CoV-2 Proteases and Human Cathepsin L

Ittipat Meewan<sup>1,2</sup>, Jacob Kattoula<sup>3, ‡</sup>, Julius Y. Kattoula<sup>3, ‡</sup>, Danielle Skinner<sup>1</sup>, Pavla Fajtová<sup>1</sup>, Miriam A. Giardini<sup>1</sup>, Brendon Woodworth<sup>1</sup>, James H. McKerrow<sup>1</sup>, Jair Lage de Siqueira-Neto<sup>1</sup>, Anthony J. O'Donoghue<sup>1</sup>, and Ruben Abagyan<sup>1,\*</sup>

<sup>1</sup>Skaggs School of Pharmacy and Pharmaceutical Sciences University of California San Diego, La Jolla, California 92093, United States

<sup>2</sup>Department of Chemistry and Biochemistry University of California San Diego, La Jolla, California 92093, United States

<sup>3</sup>Biological Sciences University of California San Diego, La Jolla, California 92093, United States

\*Corresponding author

E-mail: rabagyan@health.ucsd.edu

‡These authors contributed equally to this work.

## Abstract

There are currently no FDA approved inhibitors of SARS-CoV-2 viral proteases with specific treatment for post-exposure of SARS-CoV-2. Here, we discovered inhibitors containing thiuram disulfide or dithiobis-(thioformate) tested against three key proteases in SARS CoV-2 replication including SARS CoV-2 Main Protease (Mpro), SARS CoV-2 Papain Like Protease (PLpro), and human cathepsin L. The use of thiuram disulfide and dithiobis-(thioformate) covalent inhibitor warheads was inspired by disulfiram, a currently prescribed drug commonly used to treat chronic alcoholism that at the present time is in Phase 2 clinical trials against SARS-CoV-2. At the maximal allowed dose, disulfiram is associated with adverse effects. Our goal was to find more potent inhibitors that target both viral proteases and one essential human protease to reduce the dosage and minimize the adverse effects associated with these agents. We found that compounds coded as RI175, JX 06, and RI172 are the most potent inhibitors from an enzymatic assay against SARS-CoV-2 Mpro, SARS-CoV-2 PLpro, and human cathepsin L with IC<sub>50</sub>s of 330, 250 nM, and 190 nM about 4.5, 17, and 11.5-fold more potent than disulfiram, respectively. The identified protease inhibitors in this series were also tested against SARS CoV-2 in a cell-based and toxicity assay and were shown to have similar or greater antiviral effect than disulfiram. The identified triple protease inhibitors and their derivatives are promising candidates for treatment of the Covid-19 virus and related variants.

**Keywords:** Covid19 drug candidates, Multiple protease inhibitors, Disulfiram, Thiuram disulfide, dithiobis-(thioformate), SARS-CoV-2 Main Protease, SARS-CoV-2 Papain Like Protease, Cathepsin L, Transmembrane Serine Protease 2 TMPRSS2, COVID-19

## 38 Introduction

39 The Severe acute respiratory syndrome coronavirus (SARS-CoV) and the Middle east  
40 respiratory syndrome coronavirus (MERS-CoV) are members of coronaviridae that can cause fatal  
41 respiratory diseases and are rapidly transmitted, but their outbreaks were far from pandemic in  
42 scale. In December 2019, a new coronavirus known as Severe acute respiratory syndrome  
43 coronavirus 2 (SARS-CoV-2) was identified in Wuhan China that causes coronavirus disease 2019  
44 (COVID-19)(1,2). COVID-19 has swept the world since early 2020; at the time of writing this  
45 paper over 4.5 million deaths and 188 million infections have occurred worldwide, causing a  
46 global pandemic(3). There is currently no specific small molecule drug treatment for SARS-CoV,  
47 MERS-CoV, and SARS-CoV-2. Therefore, heavy priority has been placed on finding an effective  
48 antiviral drug, and several viral targets have been considered.

49 Two important viral targets controlling the production of functional proteins by SARS-  
50 CoV-2, a positive sense RNA virus, include Main Protease (Mpro) and Papain-like Protease  
51 (PLpro) encoded by the viral genome(4). A frameshift between Open Reading Frame 1a (ORF1a)  
52 and Open Reading Frame 1b (ORF1b) enables the production of two polypeptides: Polypeptide 1a  
53 (pp1a) and Polypeptide 1b (pp1ab). The viral proteases Mpro and Plpro process pp1a and pp1ab  
54 into 16 non-structural proteins necessary for viral assembly and replication as depicted in **Fig 1**.  
55 While inhibitors of individual proteases have been suggested(5,6), there are obvious benefits from  
56 the inhibition of *both* viral proteases in order to limit overall SARS-CoV-2 viral replication.

57

58 **Figure 1. Schematic drawing of polypeptide expressed by SARS-CoV-2 including**  
59 **nonstructural proteins (NSP), structural proteins, and accessory proteins.** Each represented

60 viral protein has not been drawn to actual scale. Brown and blue arrows represent cleavage sites  
61 of SARS-CoV-2 Mpro and PLpro cleavage sites, respectively. Cathepsin L cleavage between  
62 S1/S2 subunits is represented by the green arrow. The cleavage sites of TMPRSS2 located between  
63 S1/S2 subunits and S' cleavage site in S2 subunit were indicated by magenta arrows.

64  
65 Moreover, the SARS-CoV-2 entry mechanism relies on two *human* proteases, the  
66 Transmembrane serine protease 2 (TMPRSS2) and endosomal cathepsin L to cleave the spike  
67 protein of SARS-CoV-2 which eventually binds to Angiotensin-converting enzyme 2 (ACE2),  
68 releasing the viral genome into the cytoplasm of the host cells and initiating the viral replication  
69 process(7–9). SARS-CoV-2 can exploit TMPRSS2 residing on cell membranes, facilitating their  
70 fusion. In addition to the TMPRSS2-mediated entry mechanism, SARS-CoV-2 can also utilize  
71 endosomal cathepsin L, an endosomal or lysosomal cysteine proteases(10). Cathepsin L was  
72 associated as a factor in COVID-19 compared to the uncorrelated lysosomal cysteine protease  
73 cathepsin B(11). These viral and human proteases are attractive targets for the design of anti-  
74 SARS-CoV-2 drugs. Our goal was to target *multiple* proteases that are necessary for the viral  
75 replication process with a *single* small molecule inhibitor. This approach is challenging but it may  
76 result in better antiviral drugs that are less sensitive to viral escape mutations resulting in drug  
77 resistance.

78 Several peptidomimetic compounds exhibiting effective inhibition against individual  
79 SARS-CoV-2 proteases have been identified(12–14) and many drugs have been investigated for  
80 drug repurposing for the COVID-19 treatment(15). However, our interests lie in covalent  
81 inhibitors working as multiple-target, anti-SARS-CoV-2 agents. One interesting compound is  
82 disulfiram which contains a thiuram disulfide covalent warhead at the center of the molecule.

83 Disulfiram is a currently approved drug commonly prescribed as an aversive treatment of chronic  
84 alcoholism. Disulfiram primarily acts as an irreversible inhibitor of alcohol dehydrogenase by  
85 binding to a cysteine residue within the active site. The binding disrupts the breakdown of alcohol  
86 causing the development of resistance to alcohol consumption through minor toxicity and adverse  
87 effects occurring upon consumption(16).

88 Beyond the treatment of alcoholism, the distinct structure of disulfiram, containing the  
89 thiuram disulfide covalent warhead, is viewed as a key component to the drug's activity in SARS-  
90 CoV-2 and is maintained as a point of interest in drugs targeting viral proteases. Previously,  
91 disulfiram was shown to inhibit both MERS-CoV and SARS-CoV PLpro with 14.6  $\mu\text{M}$  and 24.1  
92  $\mu\text{M}$   $\text{IC}_{50}$  values respectively. It was shown that disulfiram may act at the active site of the SARS-  
93 CoV PLpro, creating a covalent adduct with Cys112 that implied possible future uses of the drug  
94 in treatment against coronaviruses(17). More recently, disulfiram was characterized to display  
95 antiviral activity against multiple viral proteases including SARS-CoV-2 Mpro ( $\text{IC}_{50}$ : 9.35  $\mu\text{M}$ )  
96 and SARS CoV-2 PLpro ( $\text{IC}_{50}$ : 6.9  $\mu\text{M}$ ) as well as several other viral cysteine proteases(18).

97 Furthermore, disulfiram has been characterized to block the pore formation of gasdermin  
98 D (GSDMD) through covalent targeting of cysteine 191, counteracting IL- $\beta$  release and  
99 inflammation(19). In phosphoglycerate dehydrogenase (PHGDH) and caspase 1, disulfiram was  
100 covalently binds to cysteine residues which ultimately blocks the release of cytokines(20,21).  
101 Further characterized targets that have been shown to be inhibited by disulfiram are displayed in  
102 **Table 1**. With knowledge of this counteraction to inflammation and other favorable outcomes of  
103 disulfiram, it is currently in Phase 2 Clinical trials being identified as a potential therapeutic target  
104 for SARS CoV-2(22).

105           Analogues of disulfiram were tested on the SARS CoV-2 Papain Like and Main Protease to  
106 determine more effective and efficient inhibitors that take advantage of disulfiram's mechanism  
107 of binding to the cysteine residue. To maintain this cysteine binding activity, our analogues contained  
108 the thiuram disulfide or dithiobis-(thioformate), varying in the functional groups beyond this  
109 center. Through experimental results, it was discovered that most analogues had either a similar or  
110 greater percent inhibition for both SARS-CoV-2 Mpro and PLpro in comparison to that of  
111 disulfiram. With overall relatively lower IC<sub>50</sub> values, we attribute these analogues as viable triple  
112 target inhibitors of both SARS-CoV-2 proteases as well as human cathepsin L that may outperform  
113 disulfiram and warrant further testing and implementation in the clinical scene.

## 114 **Materials and methods**

### 115 **Computational modeling**

116           In our docking simulation, we obtained high resolution X-ray crystal structures of SARS-  
117 CoV-2 PLpro and Mpro from Protein Data Bank (PDB code: 5XBG and 6WX4, respectively) as  
118 the docking receptors. Protein-ligand complexes conformation and stability were determined by  
119 docking scores, which represent Gibbs free energy. The algorithm for sampling 3D conformation  
120 of ligands and pockets was generated randomly based on biased probability Monte Carlo. All  
121 docking simulations, scoring functions and pharmacokinetic properties were also predicted from  
122 ICM-Pro v3.9(23,24).

### 123 **Compounds and reagents**

124           Disulfiram was purchased from Fisher Scientific (Hampton, NH). RI171 and RI172 were  
125 purchased from MolPort (Latvia) while JX 06 was purchased from Ambeed (Arlington Heights,

126 IL). Thiram, RI175, RI176, and RI177 were obtained from Sigma-Aldrich (St. Louis, MO). All  
127 compounds were dissolved in dimethyl sulfoxide. All solvents were reagent grade, and all reagents  
128 were purchased from Sigma-Aldrich (St. Louis, MO).

## 129 **Recombinant protein and substrates**

130 The recombinant SARS-CoV-2 main protease (Mpro) was expressed using the Mpro  
131 plasmid provided by Rolf Hilgenfeld(25) and purified as previously described(12,25).  
132 Recombinant proteases were purchased from following vendors: SARS-CoV-2 PLpro (Acro  
133 Biosystems, Newark, DE), Thrombin (R & D Systems, Minneapolis, MN), TMPRSS2 (Cusabio  
134 Technology LLC, Houston, TX), and human cathepsin L (R & D Systems, Minneapolis, MN).  
135 Protease substrates were purchased from following vendors: MCA-AVLQSGFR-K(DNP)-K-NH<sub>2</sub>  
136 (R & D Systems, Minneapolis, MN), Z-RLRGG-AMC (Bachem Holding AG, Switzerland), Boc-  
137 VPR-AMC (Sigma-Aldrich, St. Louis, MO), Boc-QAR-AMC (Peptides International, Inc.,  
138 Louisville, KY), and Z-FR-AMC (R & D Systems, Minneapolis, MN)

## 139 **Enzymatic inhibition assay**

140 The protease enzymatic activities of SARS-CoV-2 Mpro and PLpro were measured using  
141 a FRET-based peptide substrate: MCA-AVLQSGFR-K(DNP)-K-NH<sub>2</sub> and fluorogenic substrate:  
142 Z-RLRGG-AMC, respectively. The protease enzymatic activities of human thrombin, human  
143 TMPRSS2, and human cathepsin L were performed using fluorogenic substrates Boc-VPR-AMC,  
144 Boc-QAR-AMC, and Z-FR-AMC, respectively.

145 SARS-CoV-2 Mpro (50 nM final concentration) enzymatic reaction was carried out in  
146 reaction buffer containing 50 mM Tris-HCl pH 7.5, 150 mM NaCl, 1 mM EDTA and 0.01% Tween  
147 20 using 10  $\mu$ M of MCA-AVLQSGFR-K(DNP)-K-NH<sub>2</sub> FRET based peptide as a substrate.

148 SARS-CoV-2 PLpro (24.46 nM final concentration) enzymatic assays were performed in reaction  
149 buffer containing 50 mM HEPES pH 6.5, 150 mM NaCl and 0.01% Tween 20 using 50  $\mu$ M of Z-  
150 RLRGG-AMC fluorogenic substrate. The positive control for these assays was 10  $\mu$ M Ebselen.  
151 Human thrombin (678.3 nM final concentration) enzymatic assays were carried out in 50 mM Tris,  
152 10 mM CaCl<sub>2</sub>, 150 mM NaCl, 0.05% Brij-35, pH 7.5 using 100  $\mu$ M Boc-VPR-AMC as the  
153 substrate and 100  $\mu$ M of dabigatran as positive control. Human TMPRSS2 (at 30 nM final  
154 concentration) was assayed in 50 mM Tris pH 8, 150 mM NaCl, and 0.01% Tween 20 buffer using  
155 10  $\mu$ M Boc-QAR-AMC substrate and 10  $\mu$ M Nafamostat as positive control. Human cathepsin L  
156 (at 1 nM) activity assay was performed in 50 mM MES, 5 mM DTT, 1 mM EDTA, and 0.005%  
157 (w/v) Brij-35, pH 6.0 using 35  $\mu$ M Z-FR-AMC as the substrate and 10  $\mu$ M of E64 as positive  
158 control. The negative controls for all assays were 0.2% DMSO. All experiments were assayed in  
159 black 384-well microplate (BD Falcon) in the total volume of 50  $\mu$ M at 37 °C. For Mpro FRET-  
160 based peptide substrate, the fluorescence signals were monitored at wavelengths of 320 and 400  
161 nm for excitation and emission, respectively. Fluorescence signals of PLpro fluorogenic substrate  
162 were monitored at wavelengths of 360 and 460 nm for excitation and emission, respectively. All  
163 fluorescence signals were detected using Synergy HTX Multi-Mode Microplate Reader (BioTek)  
164 and data were visualized using Gen5 Software (BioTek). Dose response curves of each compound  
165 against all selected proteases were performed on 10 concentrations in triplicate ranging from 50  
166 mM to 100 nM and IC<sub>50</sub> values of each compound were calculated accordingly using SciPy and  
167 Matplotlib Python packages.

## 168 **Cells culture and immunofluorescence assay**

169 For infectivity assay, Vero-E6 cells (2,000 cells/well, 384 well plate format) were used as  
170 host cells, infected with SARS-CoV-2 in an ‘multiplicity-of-infection’ value (MOI) of 1.0. Certain

171 concentrations of compounds were spotted in the plates, followed by the Vero cells. Cells were  
172 incubated overnight at 37 °C with 5% of CO<sub>2</sub>. The cells were then infected by the virus and were  
173 incubated for 48h at 37°C with 5% CO<sub>2</sub>. The plates were then fixed with 4% PFA evaluated  
174 immunofluorescence signal for viral detection using Rabbit anti-nucleocapsid (GeneTex, cat#  
175 GTX135357) and anti-Rabbit Alexa488 as a secondary antibody. Cells were counterstained with  
176 DAPI. The image signals were analyzed using MetaXpress software to quantify individual cells  
177 and infected cells.

## 178 **Results**

### 179 **SARS-CoV-2 Mpro and PLpro activity assay.**

180 Previous studies revealed that disulfiram has inhibitory activity against both Mpro and  
181 PLpro of SARS-CoV-2(18,26,27) and PLpro of SARS-CoV and MERS(16). In addition,  
182 disulfiram is currently being studied in phase two clinical trials as a therapeutic agent for SARS-  
183 CoV-2 infection(22). Disulfiram is known to form an irreversible covalent bond that targets active  
184 cysteine proteases(28). The excellent potency of disulfiram inspired us to further explore the  
185 inhibitory activities of compounds that contain thiuram disulfide or dithiobis-(thioformate), a  
186 necessary functional group for covalent binding to cysteine protease targets(29). Therefore, we  
187 selected six thiuram disulfide analogs with different N-substituents and one dithiobis-  
188 (thioformate), RI171 to RI177, to test against SARS-CoV-2 Mpro and PLpro. We performed  
189 fluorometric enzymatic assays to show the activities of Mpro and PLpro in the presence of selected  
190 compounds. The assays were performed using a FRET-based peptide substrate: MCA-  
191 AVLQSGFR-K(DNP)-K-NH<sub>2</sub> at 10 μM and fluorogenic substrate: Z-RLRGG-AMC at 50 μM for



192 Mpro and PLpro, respectively. As shown in **Fig 2** and **Table 1**, the inhibitory activities of RI172  
193 and JX 06 against Mpro with the half-maximum inhibitory concentration ( $IC_{50}$ ) of  $0.56 \pm 0.06$  and  
194  $0.63 \pm 0.13$  nM, respectively, showed approximately three folds improvement from disulfiram  
195 with an  $IC_{50}$  value of  $1.48 \pm 0.06$   $\mu$ M ( $2.1 \pm 0.3$   $\mu$ M reported value(26), while Thiram, RI171, and  
196 RI177 showed slightly weaker inhibition effects compared to disulfiram. In addition, four of the  
197 thiuram disulfide compounds, JX 06, RI172, Thiram and RI171 showed significant potency  
198 improvement against PLpro with  $IC_{50}$  of  $0.25 \pm 0.05$ ,  $0.68 \pm 0.01$ ,  $0.62 \pm 0.03$ , and  $1.93 \pm 0.06$   
199  $\mu$ M, respectively, compared to the reported  $IC_{50}$  of disulfiram,  $4.11$   $\mu$ M ( $6.9 \pm 4.2$   $\mu$ M reported  
200 value(18) especially for JX 06 which showed a 17-fold improvement over disulfiram.

201

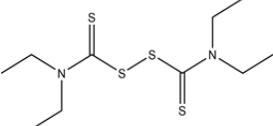
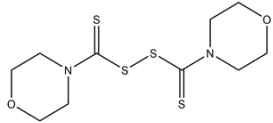
202 **Figure 2. Selected thiuram disulfide or dithiobis-(thioformate) analogues show potent**  
203 **inhibition against SARS-CoV-2 Mpro and PLpro.** Dose response curves of disulfiram, RI171,  
204 RI172, JX 06, Thiram, RI175, and RI177 against SARS-CoV-2 Mpro (blue) and PLpro (brown).  
205 Disulfiram dose response curve performed under the same conditions is shown for comparison.  
206 The proteolytic activities of both enzymes were determined by the enzymatic fluorescence assay  
207 and shown as percent activities relative to the negative control (DMSO). Error bars represent  
208 standard errors of independent three experiments.

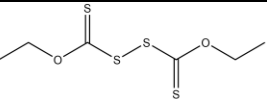
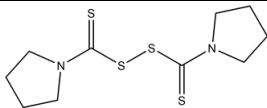
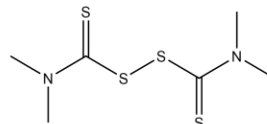
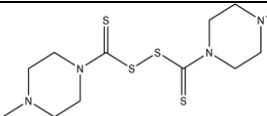
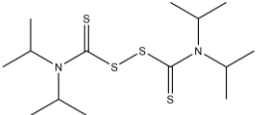
209

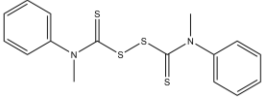
210 These results suggest that thiuram disulfide is a necessary moiety to interact covalently  
211 with cysteine active residues of Mpro and PLpro. The replacement of ethylamine groups in  
212 disulfiram with morpholine, pyrrolidine, methylamine, and 4-methylpiperazine in JX 06, RI172,  
213 Thiram, and RI171, respectively, moderately enhance the potency of inhibitors against Mpro and

214 PLpro, while substitution by isopropylamine in RI177 showed the preservation of inhibition of  
215 Mpro but completely lost the inhibitory activity ( $IC_{50} > 50 \mu M$ ) against PLpro. Furthermore, the  
216 presence of N-methylaniline moiety in RI177 entirely lost the inhibition potency ( $IC_{50} > 50 \mu M$ )  
217 in both Mpro and PLpro. These results suggest that the substitution of bulky and flat moieties at  
218 terminal N-substituents are unfavorable for the improvement of inhibition against SARS-CoV-2  
219 proteases for thiuram disulfide analogues. It is especially interesting that RI175 which contains  
220 dithiobis-(thioformate), unlike the rest of the compounds in this series, has shown potent inhibitory  
221 activity against both Mpro and PLpro,  $0.33 \pm 0.06$  and  $0.64 \pm 0.06 \mu M$ , respectively.

**Table 1-1.** Structures of tested compounds with their known targets and enzymatic assays against SARS-CoV-2 Mpro and PLpro investigated in this study.

Entry	Compounds name	Structure	Previously Characterized Targets	SARS-CoV-2 Proteases Targets		Human Protease Target
				Mpro IC <sub>50</sub> (μM)	PLpro IC <sub>50</sub> (μM)	Cathepsin L IC <sub>50</sub> (μM)
1	Disulfiram		SARS-CoV-2 main and papain-like proteases (Mpro and PLpro)(18) Aldehyde dehydrogenase 2 (ALDH2) <sup>27</sup> Dopamine beta hydroxylase (DBH) <sup>15</sup> Gasdermin D (GSDMD) <sup>18</sup> Pyruvate Dehydrogenase Kinase 1 (PDK1)(30) Ubiquitin E3 Ligase Breast Cancer Associated Protein 2 (BCA2)(31)	1.48±0.06	3.84±0.05	2.19±1.36
2	JX 06 di-Morpholine-thiuram disulfide		Gasdermin D (GSDMD)(19) Pyruvate Dehydrogenase Kinase 1 (PDK1)(30) Human Monoacylglycerol Lipase (hMGL)(32)	0.56±0.06	0.25±0.05	1.65±0.64

Entry	Compounds name	Structure	Previously Characterized Targets	SARS-CoV-2 Proteases Targets		Human Protease Target
				Mpro IC <sub>50</sub> (μM)	PLpro IC <sub>50</sub> (μM)	Cathepsin L IC <sub>50</sub> (μM)
3	RI175 O,O-di-Ethyl dithiobis- thioformate			<b>0.33±0.06</b>	<b>0.64±0.06</b>	<b>1.91±0.62</b>
4	RI172 di-Pyrrolidine- thiuram disulfide		Human Monoacylglycerol Lipase (hMGL)(32)  Ubiquitin E3 Ligase Breast Cancer  Associated Protein 2 (BCA2)(31)	<b>0.63±0.13</b>	<b>0.68±0.01</b>	<b>0.19±0.03</b>
5	Thiram tetra-Methyl- thiuram disulfide (Thiram)		Pyruvate Dehydrogenase Kinase 1 (PDK1)(30)	<b>1.95±0.29</b>	<b>0.62±0.03</b>	16.86±6.87
6	RI171 di-4- Methylpiperazin e-thiuram disulfide		Human Monoacylglycerol Lipase (hMGL)(32)  Ubiquitin E3 Ligase Breast Cancer  Associated Protein 2 (BCA2)(31)	<b>3.24±0.06</b>	<b>1.93±0.06</b>	4.54±0.67
7	RI177 tetra-IsoPropyl- thiuram disulfide			<b>3.81±0.55</b>	>50	>50

Entry	Compounds name	Structure	Previously Characterized Targets	SARS-CoV-2 Proteases Targets		Human Protease Target
				Mpro IC <sub>50</sub> (μM)	PLpro IC <sub>50</sub> (μM)	Cathepsin L IC <sub>50</sub> (μM)
8	RI176 di-Methyl-di-Phenyl-thiuram disulfide			>50	>50	>50

## 222 **Cell entry proteins inhibition.**

223           Beside Mpro and PLpro, there are host proteases including TMPRSS2, cathepsin L, and  
224 furin that are necessary for SARS-CoV-2 viral replication. We selected both the endosomal  
225 cathepsin L and TMPRSS2 proteases that facilitate viral entry into the cell. SARS-CoV-2 binds to  
226 ACE2 on the cell surface and can enter cells either by single or dual activation mechanisms from  
227 Cathepsin L in the endosome and TMPRSS2 on the cell surface(10,33). In the previous section,  
228 several selected thiuram disulfide or dithiobis-(thioformate) analogues have shown excellent  
229 broadened inhibitory activity against both SARS-CoV-2 viral proteases. The mechanism of action  
230 of thiuram disulfide or dithiobis-(thioformate) analogues were known to bind to sulfhydryl groups  
231 of cysteine active residues of Mpro and PLpro becoming their oxidized cysteine form (**Fig 3**).  
232 Since cathepsin L contains cysteine as an active residue similar to Mpro and PLpro(34,35), we  
233 tested whether these compounds could also target cathepsin L, perhaps providing small molecules  
234 that target multiple key proteins for the viral replication process, producing a more favorable  
235 outcome for SARS-CoV-2 treatment. Thus, we also evaluated the inhibition activity of the selected  
236 compounds against 1 nM of cathepsin L using 30  $\mu$ M of Z-Phe-Arg-AMC as a fluorogenic  
237 substrate; the dose response curves of each compound are shown in **Fig 4**. IC<sub>50</sub> values of  
238 compounds JX 06 and RI175 (1.65 and 1.91  $\mu$ M) have shown slight improvement from disulfiram  
239 (2.19 $\pm$ 1.36  $\mu$ M). RI172 showed excellent potency (0.19 $\pm$ 0.03  $\mu$ M) and significant enhancement,  
240 approximately 11.5 times more potent than disulfiram. Compounds RI171 and Thiram exhibited  
241 less potency compared to disulfiram, but they are still in acceptable range. On the other hand,  
242 thiuram disulfide analogs connected to bulky substituents isopropyl and methyl-di-phenyl, RI176  
243 and RI177, respectively, did not seem to have any inhibitory effect to cathepsin L. This suggests

244 that small alkyl or heterocyclic substituents on thiuram disulfide or dithiobis-(thioformate) analogs  
245 are more favorable than bulky substituents for strong inhibition to cathepsin L.

246

247 **Figure 3. Binding conformation of thiuram disulfide or dithiobis-(thioformate).** **A.** The  
248 mechanism of RI172 when it covalently reacts to active cysteine residue of SARS-CoV-2 Mpro  
249 and PLpro. **B.** Predicted 3D conformation of RI172 shown in orange stick in SARS-CoV-2 Mpro  
250 surrounded by catalytic dyads active residues Cys145 and His41. **C.** Predicted 3D conformation  
251 of RI172 shown in orange stick in SARS-CoV-2 PLpro surrounded by catalytic triads active  
252 residues Cys111, His272, and Asp286

253 **Figure 4. Thiuram disulfide or dithiobis-(thioformate) analogues inhibit human cathepsin L.**  
254 Dose response curves of newly identified dual viral protease inhibitors disulfiram, RI171, RI172,  
255 JX 06, Thiram, RI175, RI176 and RI177 against human protease cathepsin L. Error bars represent  
256 standard errors of independent three experiments. The proteolytic activities of both enzymes were  
257 determined by the enzymatic fluorescence assay and shown as percent activities relative to the  
258 negative control (DMSO).

259

260 However, inactivation of cathepsin L does not completely prevent viral entry into the cell  
261 as SARS-CoV-2 utilizes TMPRSS2 as an alternative entry pathway(10). We tested our compounds  
262 against 30 nM of human TMPRSS2 using fluorogenic substrate 100  $\mu$ M Boc-Gln-Ala-Arg-AMC,  
263 however there was no inhibitory activity of any compound up to 100  $\mu$ M (**Fig S1**). This proposes  
264 a cysteine protease specificity of the thiuram disulfide or dithiobis-(thioformate) analogues.

265 According to these results, we have found triple inhibitors that target SARS-CoV-2 Mpro, SARS-  
266 CoV-2 PLpro, and human cathepsin L.

### 267 **Indirect effect in COVID-19 treatment through inhibition of Thrombin.**

268 Previously, it was shown that all thiuram disulfide or dithiobis-(thioformate) compounds  
269 have high potency against Mpro and PLpro of SARS-CoV-2 and human cathepsin L. Yet, we  
270 desired to further investigate if these compounds also inhibited other proteases related to the  
271 SARS-CoV-2 infection to provide further benefits in COVID-19 treatment. Severe pneumonia,  
272 acute inflammation and blood clots are common complications found in some severe COVID-19  
273 infections(36–39). Coagulation is the usual immune response to bacterial or viral infections.  
274 However, COVID-19 is typically associated with hyper-inflammation activated by cytokines  
275 including interleukin-6 (IL-6), interleukin-1 (IL-1), and tumor necrosis factor- $\alpha$  (TNF- $\alpha$ ) which  
276 can cause severe inflammation and harmful tissue damage if they were produced in excessive  
277 amount(40). Thrombin is a key protease for blood clot initialization by conversion coagulation  
278 factor from fibrinogen to fibrin. During inflammation, the anti-coagulation mechanism that  
279 prevents too much thrombin activation sometimes fails due to hyper-inflammation. This effect can  
280 increase risk of microthrombosis. Here, we tested if our selected compounds could slow down this  
281 hypercoagulation. However, when tested against 1 nM thrombin, even a 100  $\mu$ M concentration of  
282 our analogs failed to show any significant inhibition (**Fig S1**).

### 283 **SARS-CoV-2 Infectivity Cells-Based Assay**

284 Thiuram disulfide and dithiobis-(thioformate) inhibit three proteases that function in  
285 various critical stages of viral replication including viral entry and viral maturation. Targeting



286 multiple proteases may have a therapeutic advantage over drugs that inhibit a single protease as it  
287 may reduce the emergence of drug resistant mutants. Therefore, we tested these triple-target  
288 compounds in a SARS-CoV-2 Vero E6 infection model. Cells were infected with SARS-CoV-2  
289 in an MOI of 1.0 and treated with 1.4  $\mu\text{M}$ , 6.0  $\mu\text{M}$  and 24  $\mu\text{M}$  of thiuram disulfide or dithiobis-  
290 (thioformate) for 48 h. We employed an immunofluorescence technique to visualize the number  
291 of viruses and host cells in the presence of these inhibitors. The half maximal effective concentration  
292 ( $\text{EC}_{50}$ ) and cytotoxic concentration ( $\text{CC}_{50}$ ) was determined (**Fig 5**). The relative antiviral activity  
293 was normalized to the untreated control (0% inhibition) and non-infected control (100%  
294 inhibition). The relative cell viability was calculated based on the number of host cells relative to  
295 the average number of untreated cells (100% cells viability). Consistent with the previous  
296 enzymatic activity results, JX 06, Thiram, RI171, RI172, RI175, and RI177 exhibited the  $\text{EC}_{50}$  in  
297 cells-based infectivity assay ranging from 2.5 to 12.6  $\mu\text{M}$ . Our best compound from three protease  
298 *in vitro* assays, JX 06, showed the lowest  $\text{EC}_{50}$  at 2.5  $\mu\text{M}$  which is approximately a *3.6-fold*  
299 *improvement compared to disulfiram*. Most compounds also exhibited acceptable range of  
300 therapeutic index values that allows the choice of appropriate concentrations for the treatment.  
301 These results provide the proof of concept of targeting multiple functional proteins involving the  
302 SARS-CoV-2 viral replication for the improvement of COVID-19 treatment.

303

304 **Figure 5. Selected thiuram disulfide or dithiobis-(thioformate) analogs reduce number of**  
305 **SARS-CoV-2 in certain concentrations.** The antiviral activity (black solid circle) against SARS-  
306 CoV-2 and cell viability (solid red square) of disulfiram, RI171, RI172, JX 06, Thiram, RI175,  
307 and RI177 at 1.4, 6, 24  $\mu\text{M}$  obtained from immunofluorescence signal and normalized compared  
308 to untreated control (0% inhibition) and non-infected control (100% inhibition and 100% cells

309 viability). The half maximal effective concentration ( $EC_{50}$ ) and cytotoxic concentration ( $CC_{50}$ ) of  
310 each compound were evaluated from antiviral efficacy and cell viability normalized signals.  
311 Suggested therapeutic concentration range were shown in light blue area where the antiviral  
312 activity and cells viability are above 60%. Fitting was performed using GraphPad Prism software.

313

## 314 **Discussion**

315 No effective therapy has been discovered for treatment of COVID-19 since the onset of the  
316 global pandemic. Treatment of COVID-19 has relied on available approved medicines such as  $\alpha$ -  
317 interferon, the anti-HIV medication lopinavir, ritonavir, and remdesivir(41). More specific and  
318 effective therapies are necessary for post infection treatment. Most antiviral research is focused on  
319 specific single target inhibitors. On the other hand, targeting multiple proteins that function in viral  
320 replication can prevent the reduction of drug effectiveness caused by mutations of different target  
321 domains to develop drug resistance mutants. Disulfiram has been identified as a potent SARS-  
322 CoV-2 Mpro and PLpro inhibitor and is currently in phase two of clinical trials study for COVID-  
323 19 treatment. Moreover, disulfiram also covalently targets multiple enzymes including aldehyde  
324 dehydrogenase (ALDH2), dopamine beta hydroxylase (DBH), gasdermin D (GSDMD), pyruvate  
325 dehydrogenase kinase 1 (PDK1), ubiquitin E3 ligase breast cancer associated protein 2 (BCA2),  
326 human monoacylglycerol lipase (hMGL), and human cathepsin L(18–20,31,42). A multi-target  
327 pharmacological approach against enzymes that are directly and indirectly associated with SARS-  
328 CoV-2 infection may improve treatment of severe viral infection and reduce the emergence of  
329 drug-resistant variants. Here, we have shown that the five selected thiuram disulfide or dithiobis-  
330 (thioformate) analogs of disulfiram target key proteases in SARS-CoV-2 replication, namely the

331 viral Mpro and PLpro enzymes in addition to human cathepsin L. We found that these compounds  
332 improve the inhibitory effectiveness against Mpro, PLpro, and cathepsin L 4.5, 17, and 11.5 times  
333 greater when compared to disulfiram, respectively. The cells-based infectivity assays also  
334 confirmed the efficacy of selected thiuram disulfide or dithiobis-(thioformate) compounds in viral  
335 infection treatment, especially for JX 06, our best compound, which showed 3.6 times more  
336 effectivity compared to disulfiram within the acceptable range of the therapeutic index. Although  
337 the suggested compounds could not cover all viral entry inhibition, a combination therapy with  
338 TMPRSS2 inhibitors such as nafamostat, camostat, and gabexate mesilate could improve the  
339 treatment efficacy in patients who have COVID-19. Beside targeting SARS-CoV-2 Mpro and  
340 PLpro, human cathepsin L, and alcohol dehydrogenase, disulfiram and JX 06, our best compound,  
341 is a known inhibitor of Pyruvate Dehydrogenase Kinase 1 (PDK1)(30) which functions as a switch  
342 from mitochondrial respiration to aerobic glycolysis. This process is called the “Warburg effect”  
343 and is thought to enhance malignancy<sup>40,41</sup>. SARS-CoV-2, similar to MERS-CoV, has a replication  
344 process that is promoted by the Warburg Effect via increasing the production of required resources  
345 for viral replication during the aerobic glycolysis enhancement(43,44). By blocking the activity of  
346 PDK1, JX 06 and all other thiuram disulfide or dithiobis-(thioformate) compounds in this series  
347 will help diminish SARS-CoV-2 viral replication, favorable for COVID-19 treatment. In addition,  
348 for most COVID-19 patients, there is extremely high production of proinflammatory cytokines  
349 that in excessive amounts can lead to acute lung injury and death<sup>42,43</sup>. Thiuram disulfide in  
350 disulfiram has been shown to covalently target Cys191 of Gasdermin D (GSDMD) and Cys116 of  
351 Phosphoglycerate dehydrogenase (PHDH) which reduce the release of inflammatory  
352 cytokines(19,45). It can be assumed that dithiobis-thioformated analogues should have consistent  
353 effect in inhibition of GSDMD and PHDH, like disulfiram. Treating COVID-19 patients with

354 thiuram disulfide or dithiobis-(thioformate) analogues not only directly inhibits Mpro and PLpro  
355 viral proteins but could also benefit indirectly via disruption of viral replication processes and the  
356 reduction of excess inflammatory cytokines through PDK1, GSMD, and PHDGH inhibition. Even  
357 though there are concerns that disulfiram might be nonspecific towards cysteine proteases and  
358 might cause numerous side effects(18), the excellent improvement of the selected thiuram disulfide  
359 or dithiobis-(thioformate) compounds compared to disulfiram against the key proteins associated  
360 with COVID-19 suggest the potential for these drugs for oral administration in lower concentration  
361 against the virus.

## Conclusions

362 A single chemical substance may specifically inhibit both two viral proteases, Mpro and  
363 PLpro, and at least one human protease involved in viral infectivity cycle. This compound may  
364 also be relatively specific to the chosen viral and host targets. We identified the derivative of  
365 thiuram disulfide or dithiobis-(thioformate) which those favorable properties with the potential to  
366 slow down the viral infectivity cycle and modulate inflammatory responses.

## Acknowledgements

367 Authors would like to thank Elany Barbosa Da Silva, Ph.D. for her help in protease assay  
368 development, and Conall Sauvey for useful discussions and assistance. R.A. thanks NIGMS for  
369 the funding support R35 GM131881.

370

371

## Authors contributions

372

373 The research was designed and supervised by R.A., A.J.O., J.L.N-S., and J.H.M. The

374 concept of hitting multiple proteins with the single compound was conceptualized by R.A.

375 Disulfiram was proposed as the reference compound by R.A. Experiments were performed by

376 I.M., D.S., P.F., M.A.G., and B.W. The manuscript was written by I.M., R.A., J.K., and J.Y.K.

377

## References

- 378 1. Tu Y-F, Chien C-S, Yarmishyn AA, Lin Y-Y, Luo Y-H, Lin Y-T, et al. A Review of  
379 SARS-CoV-2 and the Ongoing Clinical Trials. *Int J Mol Sci.* 2020 Apr 10;21(7).
- 380 2. The species Severe acute respiratory syndrome-related coronavirus: classifying 2019-nCoV  
381 and naming it SARS-CoV-2. *Nat Microbiol.* 2020 Apr;5(4):536–44.
- 382 3. Ritchie H, Ortiz-Ospina E, Beltekian D, Mathieu E, Hasell J, Macdonald B, et al.  
383 Coronavirus Pandemic (COVID-19). *Our World in Data* [Internet]. 2020; Available from:  
384 <https://ourworldindata.org/coronavirus>
- 385 4. Chen Y, Liu Q, Guo D. Emerging coronaviruses: Genome structure, replication, and  
386 pathogenesis. *J Med Virol.* 2020 Apr;92(4):418–23.
- 387 5. Hung H-C, Ke Y-Y, Huang SY, Huang P-N, Kung Y-A, Chang T-Y, et al. Discovery of M  
388 Protease Inhibitors Encoded by SARS-CoV-2. *Antimicrob Agents Chemother.* 2020 Aug  
389 20;64(9).
- 390 6. Ma C, Sacco MD, Xia Z, Lambrinidis G, Townsend JA, Hu Y, et al. Discovery of SARS-  
391 CoV-2 Papain-like Protease Inhibitors through a Combination of High-Throughput  
392 Screening and a FlipGFP-Based Reporter Assay. *ACS Cent Sci* [Internet]. 2021 Jun 18;  
393 Available from: <https://doi.org/10.1021/acscentsci.1c00519>
- 394 7. Shang J, Wan Y, Luo C, Ye G, Geng Q, Auerbach A, et al. Cell entry mechanisms of  
395 SARS-CoV-2. *Proc Natl Acad Sci U S A.* 2020 May 26;117(21):11727–34.
- 396 8. Mahmoud IS, Jarrar YB, Alshaer W, Ismail S. SARS-CoV-2 entry in host cells-multiple  
397 targets for treatment and prevention. *Biochimie.* 2020 Aug;175:93–8.

- 398 9. Murgolo N, Therien AG, Howell B, Klein D, Koeplinger K, Lieberman LA, et al. SARS-  
399 CoV-2 tropism, entry, replication, and propagation: Considerations for drug discovery and  
400 development. *PLoS Pathog.* 2021 Feb;17(2):e1009225.
- 401 10. Ou T, Mou H, Zhang L, Ojha A, Choe H, Farzan M. Hydroxychloroquine-mediated  
402 inhibition of SARS-CoV-2 entry is attenuated by TMPRSS2. *PLoS Pathog.* 2021  
403 Jan;17(1):e1009212.
- 404 11. Zhao M-M, Yang W-L, Yang F-Y, Zhang L, Huang W-J, Hou W, et al. Cathepsin L plays a  
405 key role in SARS-CoV-2 infection in humans and humanized mice and is a promising  
406 target for new drug development. *Signal Transduct Target Ther.* 2021 Mar 27;6(1):134.
- 407 12. Mellott DM, Tseng C-T, Drelich A, Fajtová P, Chenna BC, Kostomiris DH, et al. A  
408 Clinical-Stage Cysteine Protease Inhibitor blocks SARS-CoV-2 Infection of Human and  
409 Monkey Cells. *ACS Chem Biol.* 2021 Apr 16;16(4):642–50.
- 410 13. Dai W, Zhang B, Jiang X-M, Su H, Li J, Zhao Y, et al. Structure-based design of antiviral  
411 drug candidates targeting the SARS-CoV-2 main protease. *Science.* 2020 Jun  
412 19;368(6497):1331–5.
- 413 14. Zhang L, Lin D, Kusov Y, Nian Y, Ma Q, Wang J, et al.  $\alpha$ -Ketoamides as Broad-Spectrum  
414 Inhibitors of Coronavirus and Enterovirus Replication: Structure-Based Design, Synthesis,  
415 and Activity Assessment. *J Med Chem.* 2020 May 14;63(9):4562–78.
- 416 15. Bakowski MA, Beutler N, Wolff KC, Kirkpatrick MG, Chen E, Nguyen T-TH, et al. Drug  
417 repurposing screens identify chemical entities for the development of COVID-19  
418 interventions. *Nat Commun.* 2021 Jun 3;12(1):3309.
- 419 16. Stokes M, Abdijadid S. Disulfiram [Internet]. StatPearls Publishing, Treasure Island (FL);  
420 2021. Available from: <https://www.ncbi.nlm.nih.gov/books/NBK459340/>
- 421 17. Lin M-H, Moses DC, Hsieh C-H, Cheng S-C, Chen Y-H, Sun C-Y, et al. Disulfiram can  
422 inhibit MERS and SARS coronavirus papain-like proteases via different modes. *Antiviral*  
423 *Res.* 2018 Feb;150:155–63.
- 424 18. Ma C, Hu Y, Townsend JA, Lagarias PI, Marty MT, Kolocouris A, et al. Ebselen,  
425 disulfiram, carmofur, PX-12, tideglusib, and shikonin are non-specific promiscuous SARS-  
426 CoV-2 main protease inhibitors. *BioRxiv Prepr Serv Biol.* 2020 Sep 16;2020.09.15.299164.
- 427 19. Hu JJ, Liu X, Xia S, Zhang Z, Zhang Y, Zhao J, et al. FDA-approved disulfiram inhibits  
428 pyroptosis by blocking gasdermin D pore formation. *Nat Immunol.* 2020 Jul;21(7):736–45.
- 429 20. Rodriguez AE, Ducker GS, Billingham LK, Martinez CA, Mainolfi N, Suri V, et al. Serine  
430 Metabolism Supports Macrophage IL-1 $\beta$  Production. *Cell Metab.* 2019 Apr 2;29(4):1003-  
431 1011.e4.
- 432 21. Nobel CS, Kimland M, Nicholson DW, Orrenius S, Slater AF. Disulfiram is a potent  
433 inhibitor of proteases of the caspase family. *Chem Res Toxicol.* 1997 Dec;10(12):1319–24.

- 434 22. Lee S. Disulfiram for COVID-19 (DISCO) Trial (DISCO) [Internet]. Available from:  
435 <https://www.clinicaltrials.gov/ct2/show/NCT04485130>
- 436 23. Abagyan R, Totrov M, Kuznetsov D. ICM—A new method for protein modeling and  
437 design: Applications to docking and structure prediction from the distorted native  
438 conformation. *J Comput Chem*. 1994 May 1;15(5):488–506.
- 439 24. Neves MAC, Totrov M, Abagyan R. Docking and scoring with ICM: the benchmarking  
440 results and strategies for improvement. *J Comput Aided Mol Des*. 2012 Jun;26(6):675–86.
- 441 25. Zhang L, Lin D, Sun X, Curth U, Drosten C, Sauerhering L, et al. Crystal structure of  
442 SARS-CoV-2 main protease provides a basis for design of improved  $\alpha$ -ketoamide  
443 inhibitors. *Science*. 2020 Apr 24;368(6489):409–12.
- 444 26. Sargsyan K, Lin C-C, Chen T, Grauffel C, Chen Y-P, Yang W-Z, et al. Multi-targeting of  
445 functional cysteines in multiple conserved SARS-CoV-2 domains by clinically safe Zn-  
446 ejectors. *Chem Sci*. 2020 Sep 1;11(36):9904–9.
- 447 27. Jin Z, Du X, Xu Y, Deng Y, Liu M, Zhao Y, et al. Structure of M(pro) from SARS-CoV-2  
448 and discovery of its inhibitors. *Nature*. 2020 Jun;582(7811):289–93.
- 449 28. De Sousa A. Disulfiram: Pharmacology and Mechanism of Action. In: De Sousa A, editor.  
450 Disulfiram: Its Use in Alcohol Dependence and Other Disorders [Internet]. Singapore:  
451 Springer Singapore; 2019. p. 9–20. Available from: [https://doi.org/10.1007/978-981-32-9876-7\\_2](https://doi.org/10.1007/978-981-32-9876-7_2)  
452
- 453 29. Huang Y, Xu Y, Song R, Ni S, Liu J, Xu Y, et al. Identification of the New Covalent  
454 Allosteric Binding Site of Fructose-1,6-bisphosphatase with Disulfiram Derivatives toward  
455 Glucose Reduction. *J Med Chem*. 2020 Jun 11;63(11):6238–47.
- 456 30. Sun W, Xie Z, Liu Y, Zhao D, Wu Z, Zhang D, et al. JX06 Selectively Inhibits Pyruvate  
457 Dehydrogenase Kinase PDK1 by a Covalent Cysteine Modification. *Cancer Res*. 2015 Nov  
458 15;75(22):4923–36.
- 459 31. Brahemi G, Kona FR, Fiasella A, Buac D, Soukupová J, Brancale A, et al. Exploring the  
460 structural requirements for inhibition of the ubiquitin E3 ligase breast cancer associated  
461 protein 2 (BCA2) as a treatment for breast cancer. *J Med Chem*. 2010 Apr 8;53(7):2757–  
462 65.
- 463 32. Kapanda CN, Muccioli GG, Labar G, Poupaert JH, Lambert DM.  
464 Bis(dialkylaminethiocarbonyl)disulfides as potent and selective monoglyceride lipase  
465 inhibitors. *J Med Chem*. 2009 Nov 26;52(22):7310–4.
- 466 33. Simmons G, Bertram S, Glowacka I, Steffen I, Chaipan C, Agudelo J, et al. Different host  
467 cell proteases activate the SARS-coronavirus spike-protein for cell-cell and virus-cell  
468 fusion. *Virology*. 2011 May 10;413(2):265–74.

- 469 34. Turk V, Stoka V, Vasiljeva O, Renko M, Sun T, Turk B, et al. Cysteine cathepsins: from  
470 structure, function and regulation to new frontiers. *Biochim Biophys Acta*. 2012  
471 Jan;1824(1):68–88.
- 472 35. Sosnowski P, Turk D. Caught in the act: the crystal structure of cleaved cathepsin L bound  
473 to the active site of Cathepsin L. *FEBS Lett*. 2016 Apr;590(8):1253–61.
- 474 36. Chen N, Zhou M, Dong X, Qu J, Gong F, Han Y, et al. Epidemiological and clinical  
475 characteristics of 99 cases of 2019 novel coronavirus pneumonia in Wuhan, China: a  
476 descriptive study. *Lancet Lond Engl*. 2020 Feb 15;395(10223):507–13.
- 477 37. Wang D, Hu B, Hu C, Zhu F, Liu X, Zhang J, et al. Clinical Characteristics of 138  
478 Hospitalized Patients With 2019 Novel Coronavirus-Infected Pneumonia in Wuhan, China.  
479 *JAMA*. 2020 Mar 17;323(11):1061–9.
- 480 38. Merad M, Martin JC. Pathological inflammation in patients with COVID-19: a key role for  
481 monocytes and macrophages. *Nat Rev Immunol*. 2020 Jun;20(6):355–62.
- 482 39. Levi M, Thachil J, Iba T, Levy JH. Coagulation abnormalities and thrombosis in patients  
483 with COVID-19. *Lancet Haematol*. 2020 Jun;7(6):e438–40.
- 484 40. Bantis A, Tsakalidis G, Zissimopoulos A, Kalaitzis C, Gianakopoulos S, Pitiakoudis M,  
485 et al. Can tumor necrosis factor  $\alpha$  (TNF- $\alpha$ ) and interleukin 6 (IL-6) be used as prognostic  
486 markers of infection following ureteroscopic lithotripsy and extracorporeal shock wave  
487 lithotripsy for ureteral stones? *Hell J Nucl Med*. 2015 Dec;18 Suppl 1:160.
- 488 41. Pasquereau S, Nehme Z, Haidar Ahmad S, Daouad F, Van Assche J, Wallet C, et al.  
489 Resveratrol Inhibits HCoV-229E and SARS-CoV-2 Coronavirus Replication In Vitro.  
490 *Viruses*. 2021 Feb 23;13(2).
- 491 42. Lipsky JJ, Shen ML, Naylor S. In vivo inhibition of aldehyde dehydrogenase by disulfiram.  
492 *Chem Biol Interact*. 2001 Jan 30;130–132(1–3):93–102.
- 493 43. Icard P, Lincet H, Wu Z, Coquerel A, Forgez P, Alifano M, et al. The key role of Warburg  
494 effect in SARS-CoV-2 replication and associated inflammatory response. *Biochimie*. 2021  
495 Jan;180:169–77.
- 496 44. Kindrachuk J, Ork B, Hart BJ, Mazur S, Holbrook MR, Frieman MB, et al. Antiviral  
497 potential of ERK/MAPK and PI3K/AKT/mTOR signaling modulation for Middle East  
498 respiratory syndrome coronavirus infection as identified by temporal kinome analysis.  
499 *Antimicrob Agents Chemother*. 2015 Feb;59(2):1088–99.
- 500 45. Spillier Q, Vertommen D, Ravez S, Marteau R, Thémans Q, Corbet C, et al. Anti-alcohol  
501 abuse drug disulfiram inhibits human PHGDH via disruption of its active tetrameric form  
502 through a specific cysteine oxidation. *Sci Rep*. 2019 Mar 18;9(1):4737.



## Supporting Information

503 **Figure S1. Screening on selected thiuram disulfide or dithiobis-(thioformate) compounds**  
504 **on TMPRSS2 and Thrombin.** Bar graph depicting percent inhibition of disulfiram, RI171,  
505 RI172, JX 06, Thiram, RI175, RI176 and RI177 at 0.1, 1, 10, 100  $\mu\text{M}$ , against **(A)** 1 nM  
506 Thrombin and **(B)** 10 nM TMPRSS2 compared to known inhibitors E64 and Nafamostat,  
507 respectively. Error bars represent standard errors of independent three experiments. graphs were  
508 created using GraphPad Prism software.

## Cleavage Site

### Cysteine proteases

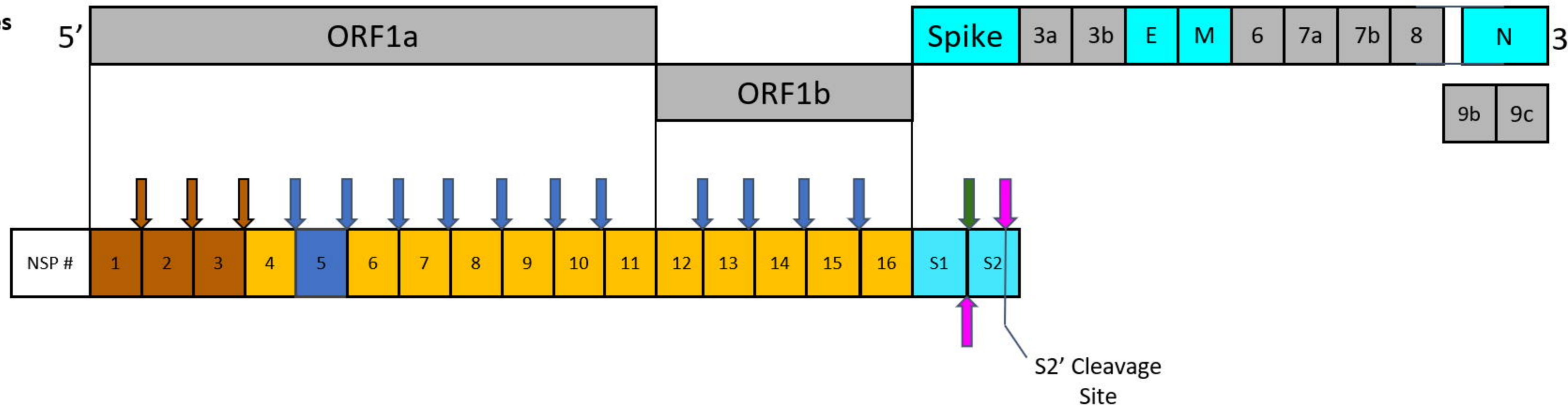


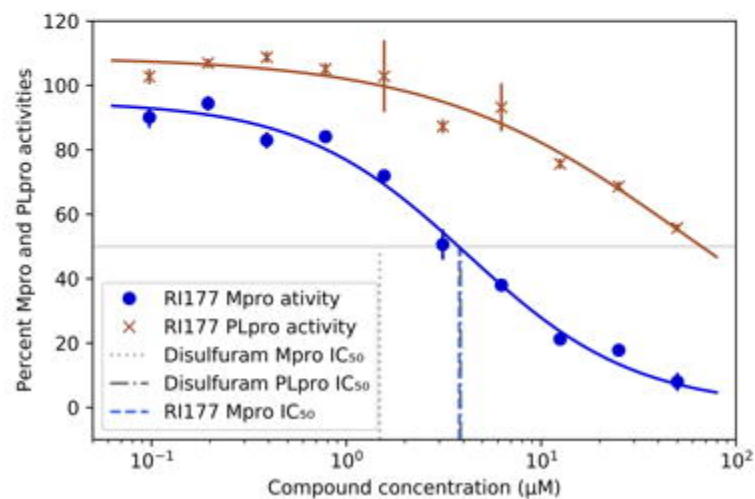
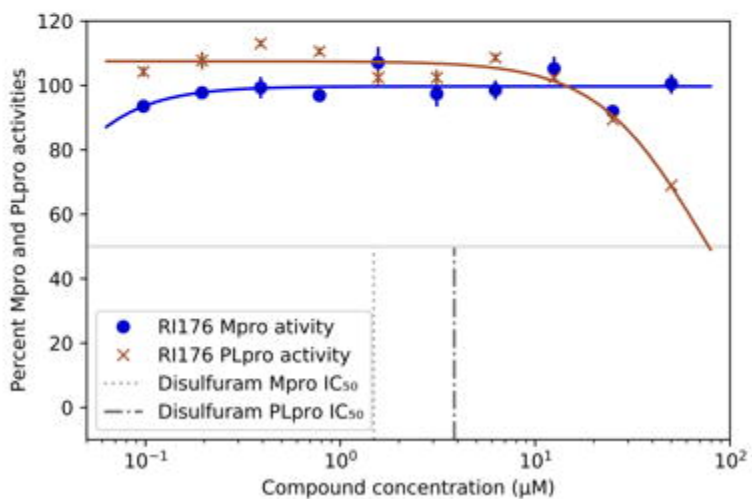
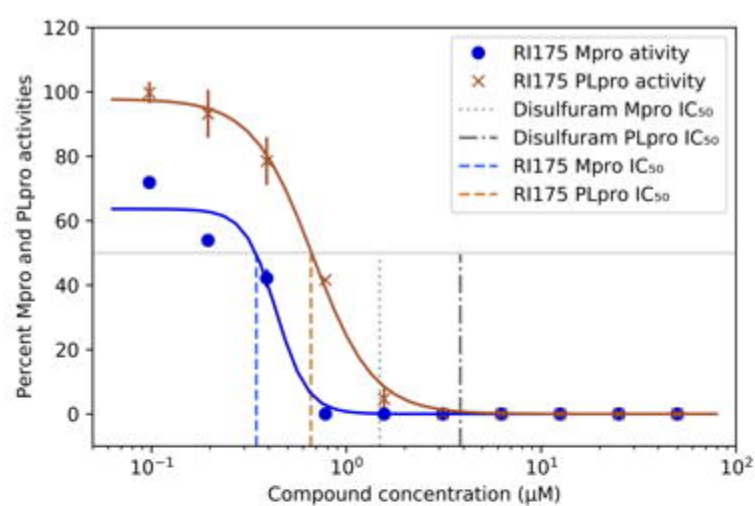
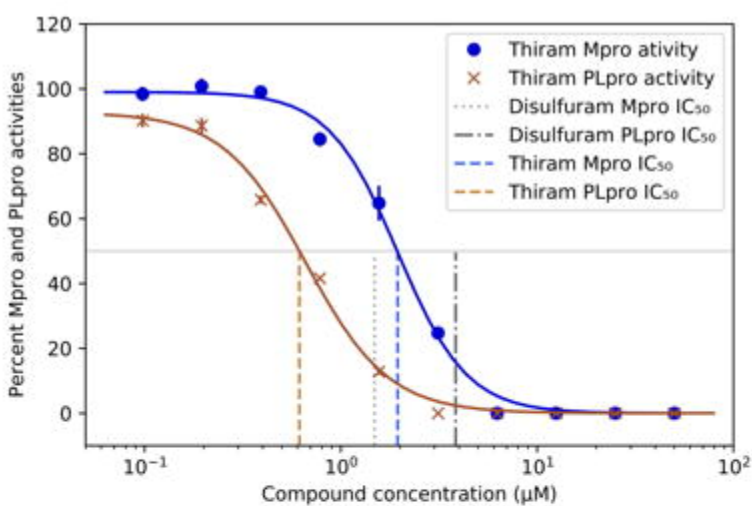
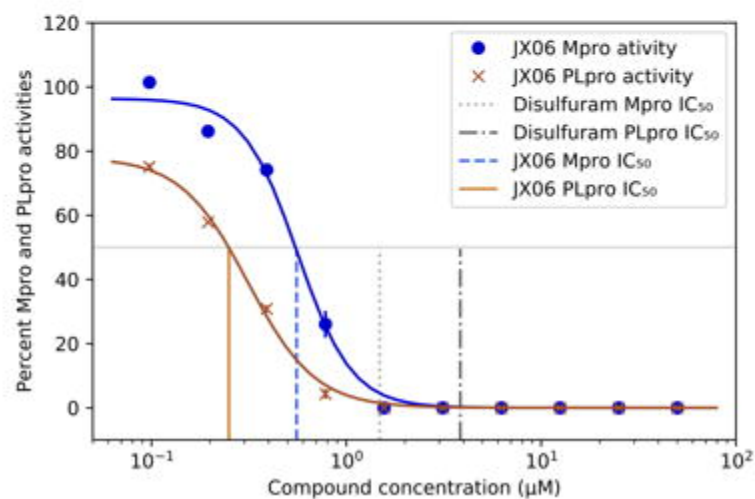
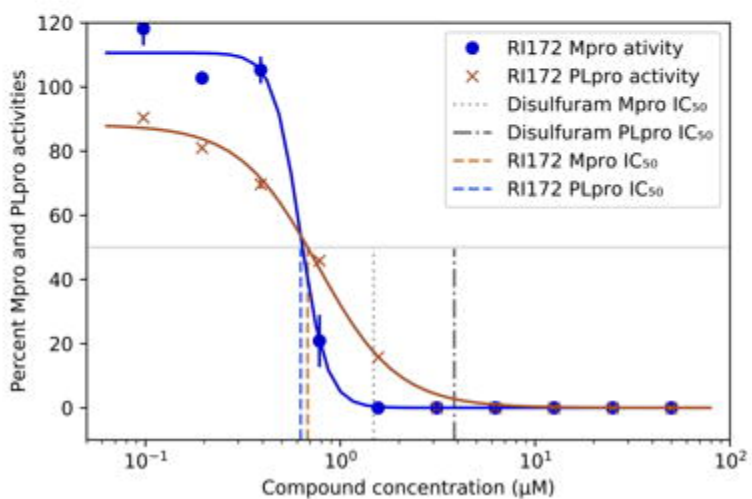
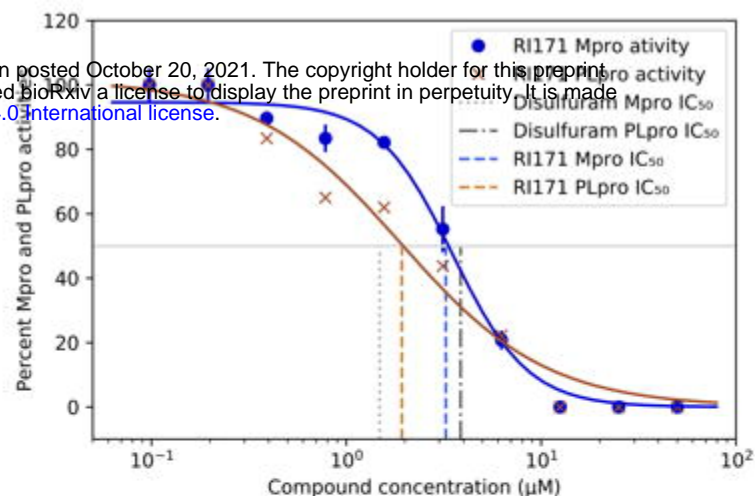
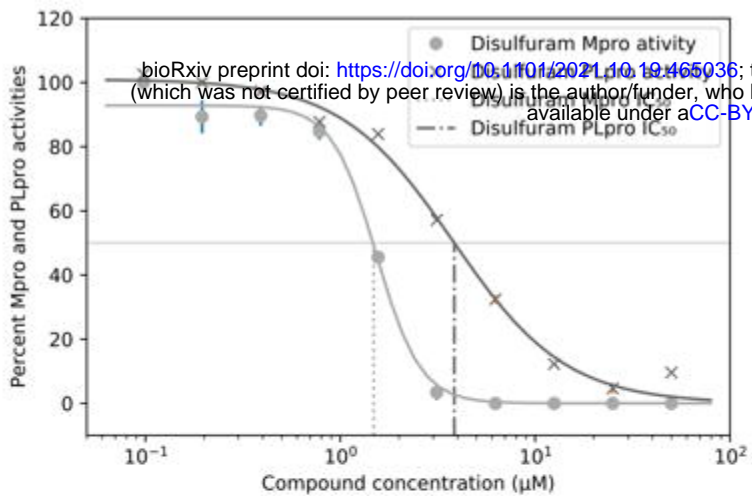
### Serine proteases



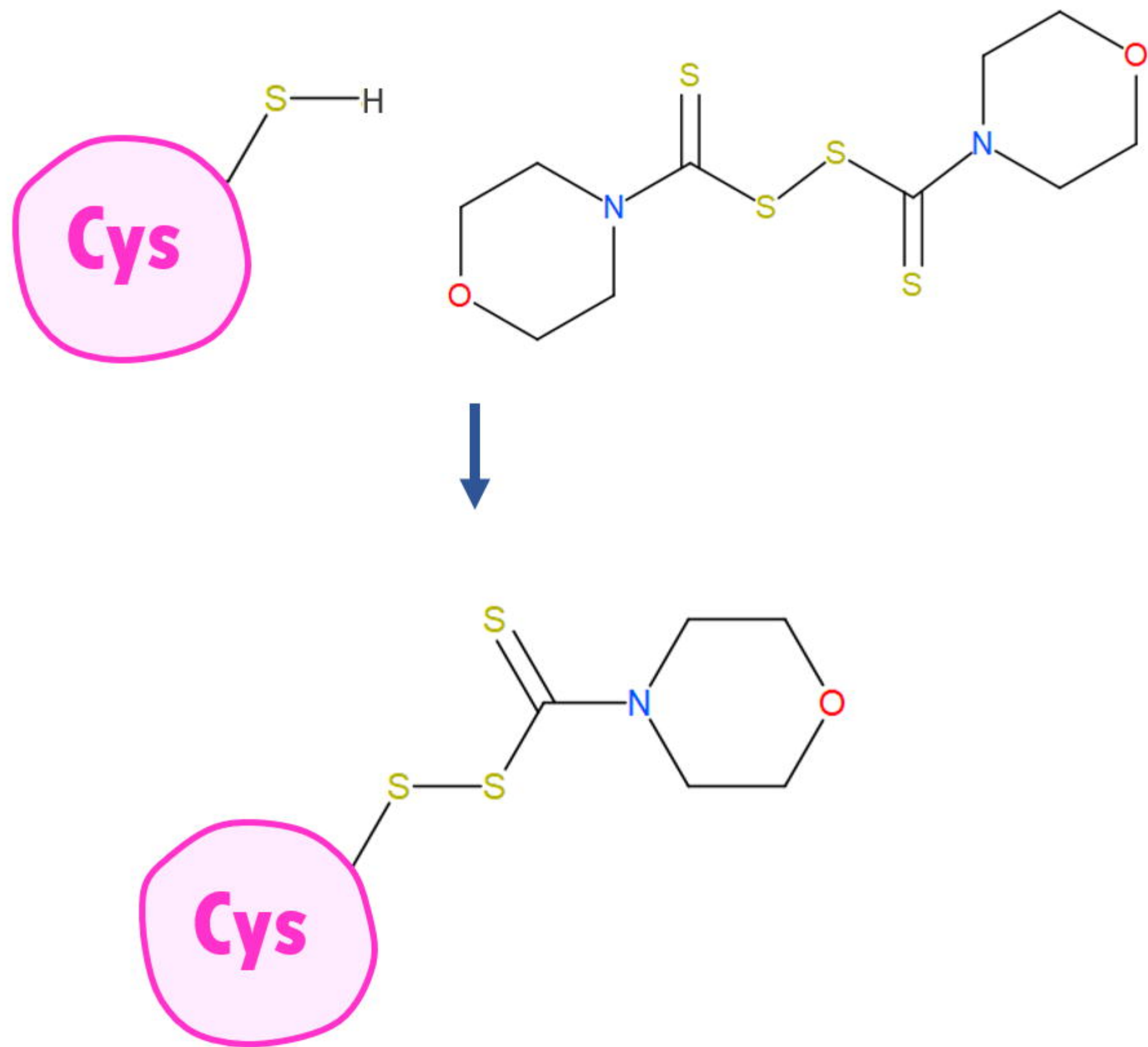
Nonstructural proteins

Structural proteins

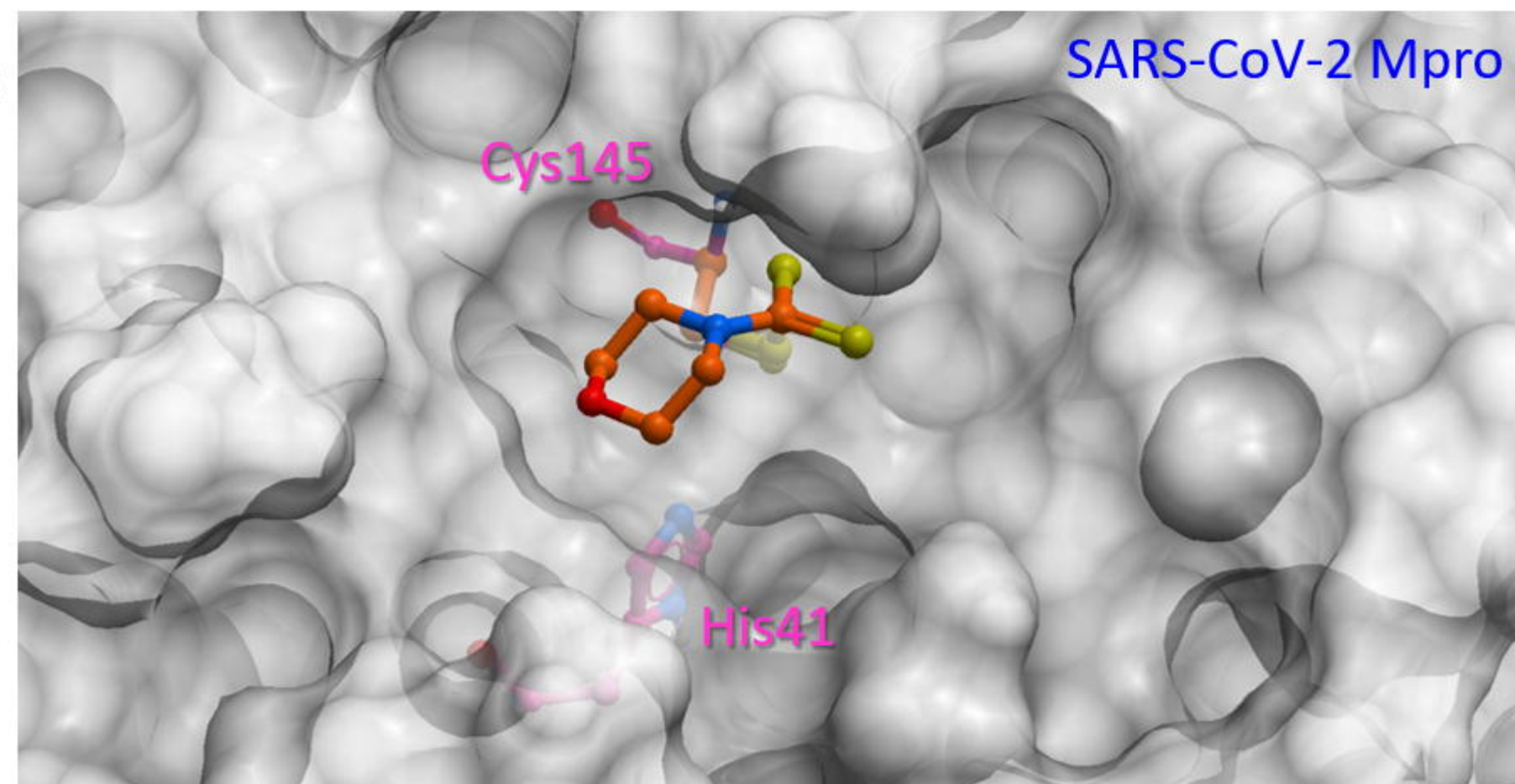




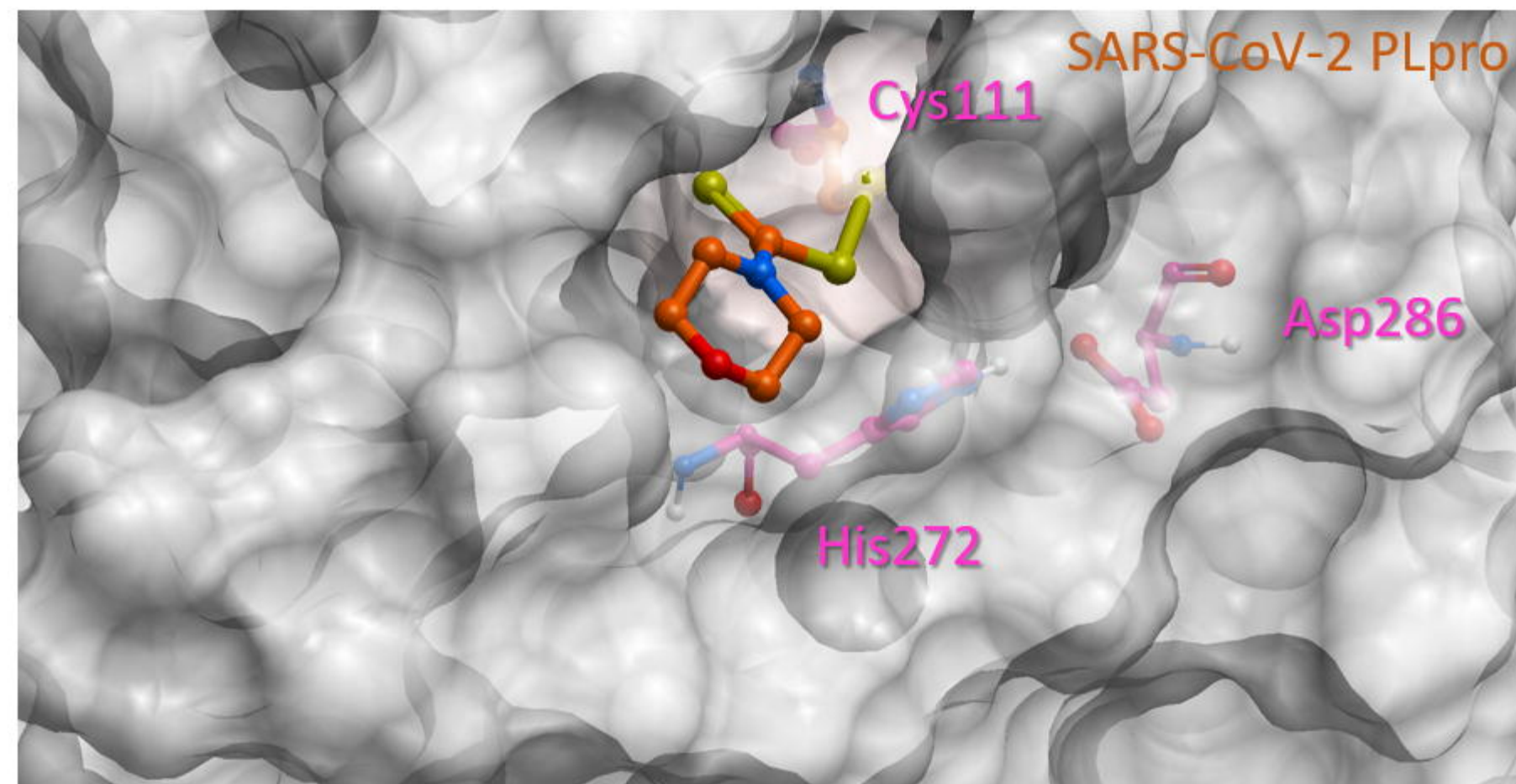
A

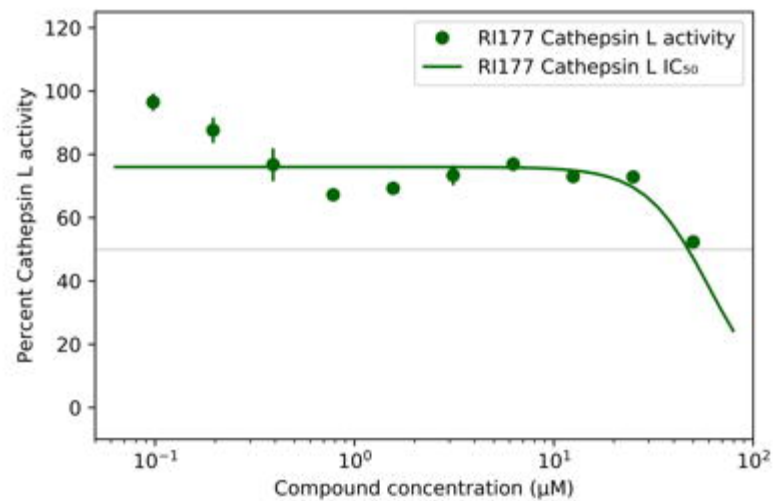
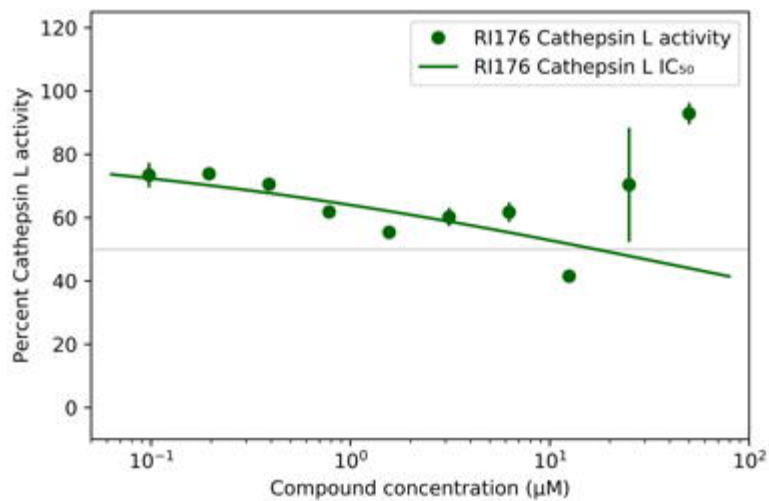
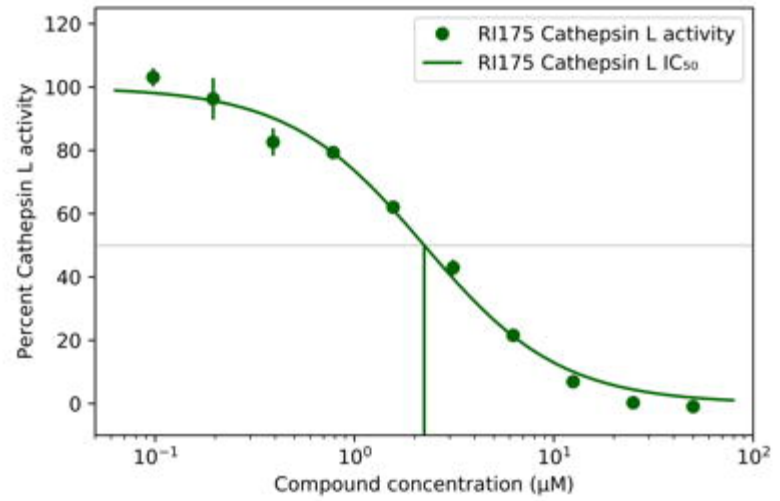
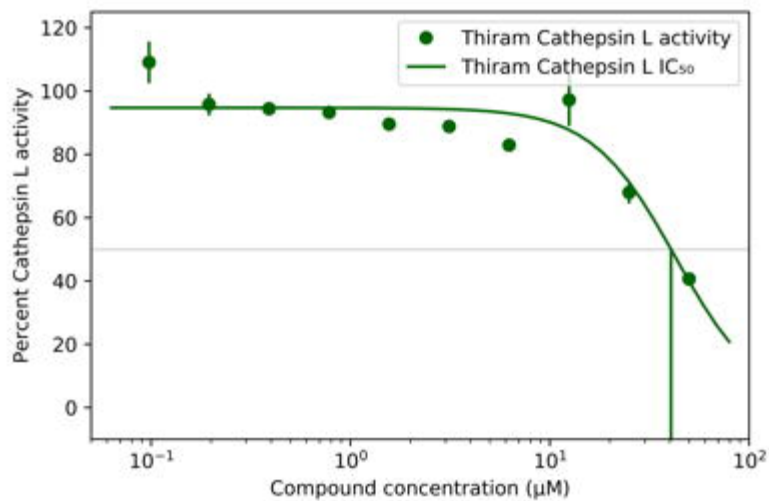
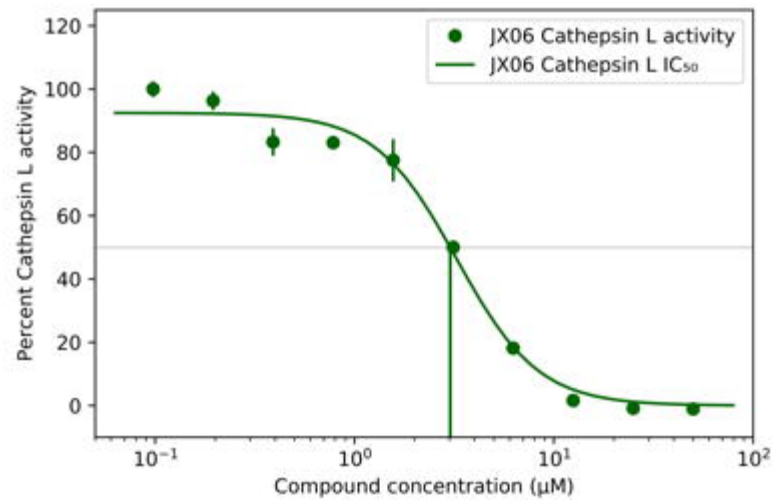
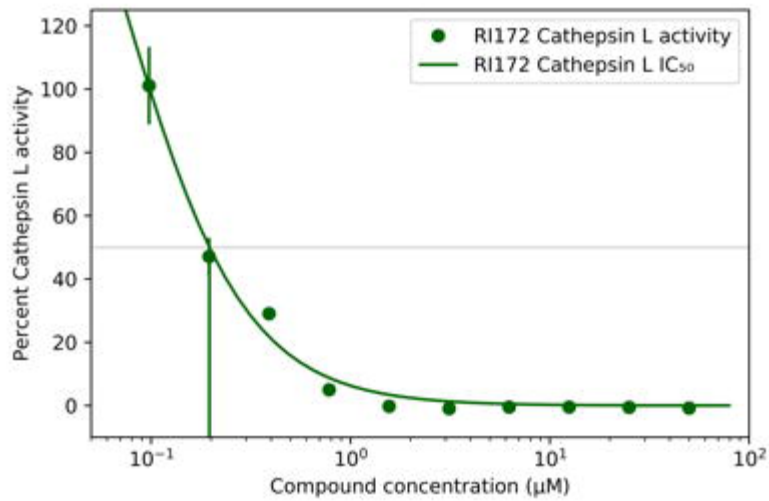
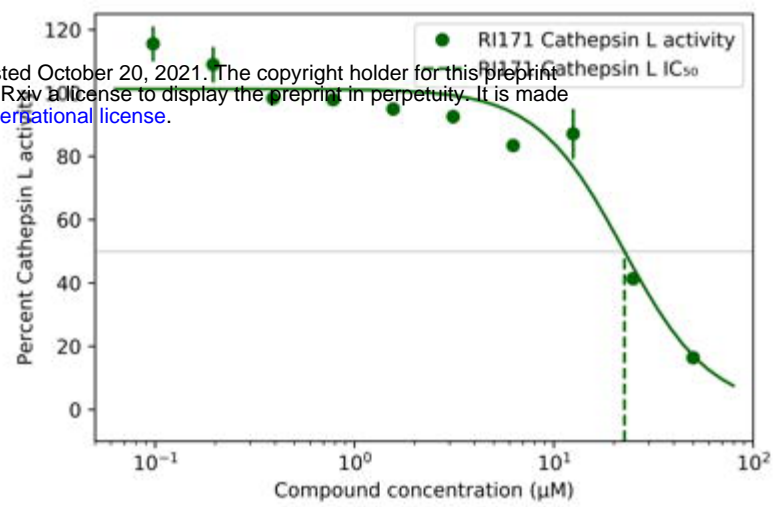
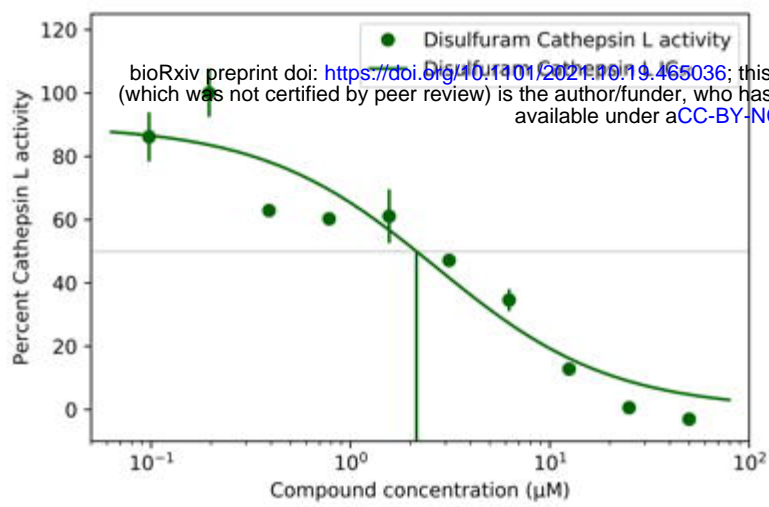


B

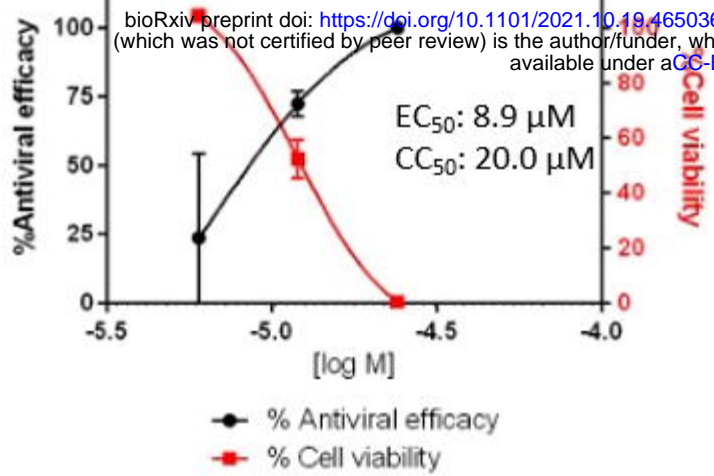


C

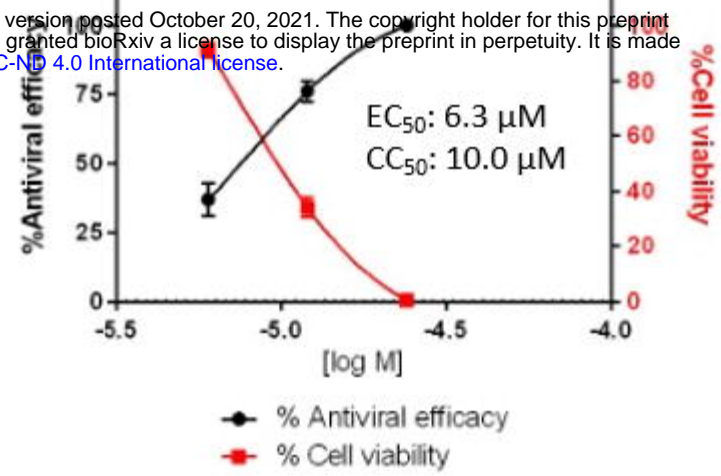




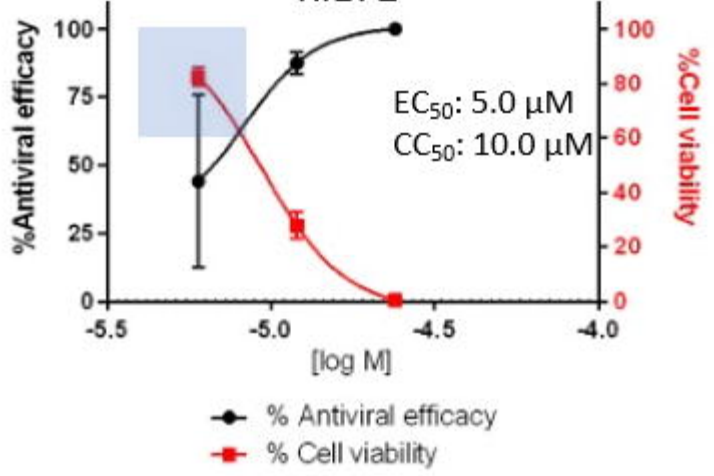
### Disulfiram



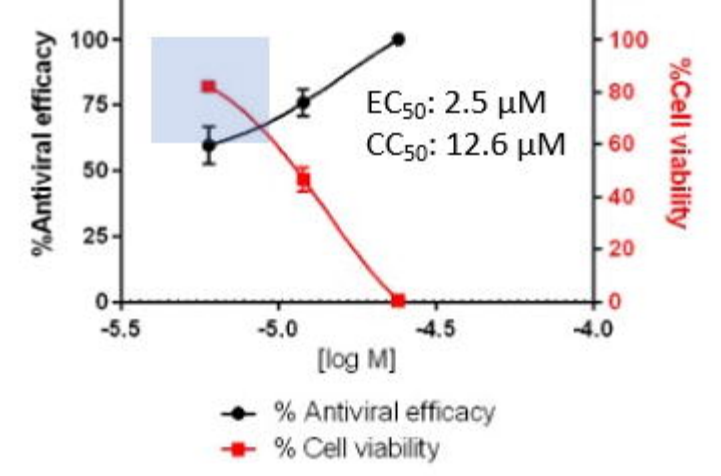
### RI171



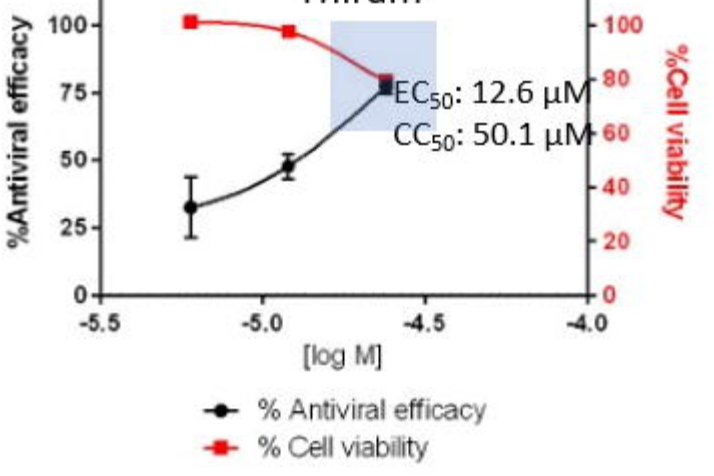
### RI172



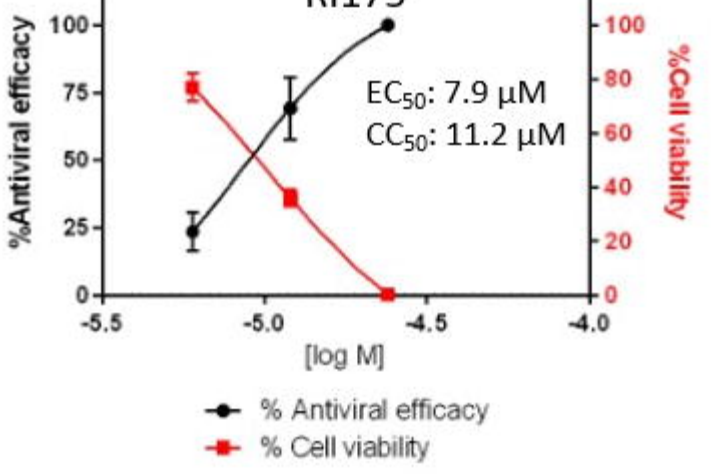
### JX 06



### Thiram



### RI175



### RI177

